journal

Microstructure/Properties Relations of Advanced Materials

J. Am. Ceram. Soc., 80 [7] 1699–705 (1997)

Ferroelasticity of t'-Zirconia: II, *In situ* Straining in a High-Voltage Electron Microscope

Bernd Baufeld,† Dietmar Baither,‡ Ulrich Messerschmidt,§ and Martin Bartsch

Max Planck Institute of Microstructure Physics, Halle (Saale), D-06120, Germany

Andreas H. Foitzik* and Manfred Rühle*

Max Planck Institute of Metals Research, Stuttgart, D-70174, Germany

The ferroelastic deformation of t'-ZrO_2, the microstructure of which was described in detail in Part I, was investigated by *in situ* deformation experiments in the high-voltage electron microscope at 1150°C. During the experiments those two domain variants with their c-axes perpendicular to the [010] tensile direction were transformed into the third one with its c-axis parallel to the tensile direction. The subsequent 'switching' of the domains inside the colonies proceeds much faster than the penetration of the transformation front into a neighboring colony. Therefore, the transformed region, exhibiting a unique tetragonal structure and containing residual defects, preferentially expands into the longitudinal directions of the colonies. The transformation of single domains proceeds instantaneously within the time resolution of the video tape recording.

I. Introduction

In the metastable material t'-zirconia, tetragonal domains fill the entire crystal volume. The microstructure is described in detail in Part I of this paper.[1] Under load, t'-ZrO_2 shows ferroelastic behavior. Very few data are available on the temperature and strain rate dependence of the coercive stress.[2–4] These data, together with a few results of the present authors, are discussed in the review paper.[5] According to this, the coercive stress strongly depends on temperature. It is probably higher than the stress for single slip on the $\langle 110 \rangle \{001\}$ slip system of cubic zirconia, but lower than the flow stress of partially stabilized zirconia (PSZ).

Ferroelastic domain switching was also observed in partially stabilized zirconia in which colonies of tetragonal domains are embedded in a homogeneous matrix.[6] According to the coercive stress and yield stress data just mentioned, ferroelastic deformation precedes dislocation plasticity, the basic mechanisms of which in untransformed PSZ are described in Refs. 7–10. If ferroelastic deformation takes place, the dislocations must move not through the original microstructure of partially stabilized zirconia, but through a microstructure changed by the ferroelastic deformation. Although the transformed areas may represent a tetragonal single crystal, they contain residual defects. The consequences of this situation are outlined in Ref. 5. In this sense, t'-zirconia may be considered a model substance to study ferroelastic deformation occurring also in other zirconia materials.

The ferroelastic deformation takes place by reorientation or switching of the tetragonal domains under the action of a suitably oriented uniaxial stress. This process proceeds by the movement of domain walls.[11] Contrary to the domain walls in ferromagnetic materials, in ferroelastic ones they are relatively thin, viz, about 5 nm in t'-ZrO_2.[12] Owing to these thin walls, domain switching should not be achieved by a simple sidewise motion of the walls as in ferromagnetics. Instead, new domains are assumed to be nucleated at the domain walls which grow two-dimensionally along the wall, with the whole process repeating until the domain is completely switched.[11,13]

To our knowledge, this process has not directly been observed up to now. Therefore, *in situ* deformation experiments in a transmission electron microscope should provide a better insight into the process of domain switching. In contrast to the uniaxial compression applied in macroscopic experiments, the *in situ* tensile deformation should result in the formation of a single domain orientation, if the tensile direction is chosen along a cube axis. The present paper describes such experiments on t'-ZrO_2.

II. Experimental Procedure

ZrO_2 single crystal specimens of 3 mol% Y_2O_3, prepared from the same material as analyzed in Part I of this paper, were used for the *in situ* experiments. The high-temperature straining stage requires microtensile samples 8 mm in length and about 2 mm in width. They are fixed to the grips of the stage by two tungsten pins in two holes of the samples. The holes are 0.5 mm in diameter and separated by 5 mm.

At first, a wire saw was used to cut slices about 0.3 mm thick from a parallelepiped with all faces orthogonal to the $\langle 100 \rangle$ pseudocubic axes. Holes were drilled by an ultrasonic drilling machine. Then, the samples were ground to a thickness of 0.1 mm on a brass plate, using a 3 μm diamond suspension. The same suspension on a polishing cloth was used for polishing. For further thinning the central region, a dimple grinder was used with a copper grinding wheel and the same diamond suspension. This dimpling is especially necessary to reduce the cross section to enable deformation by the limited force of the straining stage (15 N). To avoid fracture before ferroelastic or plastic deformation of these brittle materials, all faces of the specimens must be polished most carefully, which here was done with an alumina suspension using a cloth wheel before the samples were further thinned down using an argon ion mill at 0.3 mA gun current and 5 kV gun voltage. The final thickness of the region transparent in the electron microscope is about 0.5 μm. For *in situ* tensile straining experiments, perforation of the specimens should in any case be avoided by carefully controlling the thickness via optical thickness fringes.

Manfred Rühle—contributing editor

Manuscript No. 191587. Received August 19, 1996; approved April 8, 1997.

Presented at a Symposium on Microstructure–Property Relations of Advanced Materials, a symposium in honor of Professor Arthur Heuer's 60th birthday, held at Max-Planck-Institut für Metallforschung, Stuttgart, Germany, April 29–30, 1996.

Supported by the Deutsche Forschungsgemeinschaft (DFG).

*Member, American Ceramic Society.

†Present address: Japan Science and Technology Corporation (JFT), Nagoya 456, Japan.

‡Present address: Max Planck Institute of Metals Research, Stuttgart, D-70174, Germany.

§Author to whom correspondence is to be addressed.

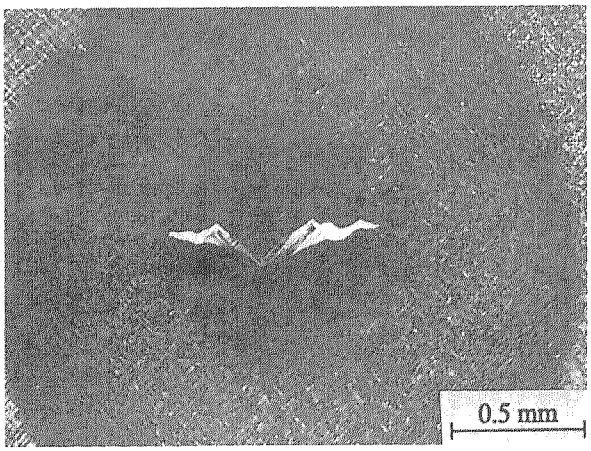

Fig. 1. Optical birefringence micrograph of a sample strained *in situ* in the HVEM. The zigzag-shaped transformed region is recognized by its homogeneous bright contrast.

The *in situ* experiments were performed at 1150°C in a specially designed double-tilting straining stage in a high-voltage electron microscope (HVEM) operated at 1000 kV. This stage is described in more detail elsewhere.[14] The [010] direction was chosen as the tensile direction. During straining, the changes of the microstructure were recorded either on photographic film or by a video system. Usually, the straining was stopped before fracture so that the details of the microstructure formed could be investigated afterwards in a wide-angle goniometer at room temperature.

III. Results

(1) Domain Switching

Changes of the microstructure owing to the ferroelastic deformation can be observed even on a macroscopic scale using optical microscopy, especially birefringence patterns, of the deformed microtensile samples after the *in situ* experiment. Before deformation, the specimens appear optically opaque. Under crossed polarizers, needlelike ⟨110⟩ oriented areas occur such as in the outer regions of Fig. 1, which was obtained from a sample strained *in situ*. The tensile direction for all micrographs is vertical on the page. While the structure is unchanged in the outer regions of the specimen, the transformation has started close to the thinnest part of the sample imaged in the middle of the figure. In this thin zone the local stress is highest, initiating the transformation process. After domain switching, the transformed region becomes transparent, turning uniformly bright under crossed polarizers. This jaggedly bound area in uniform contrast can clearly be distinguished from the outer untransformed structure. During straining, the transformed area expands, resembling crack propagation, although there is no perforation in the sample. The boundaries of the transformed region run predominantly in ⟨110⟩ directions. The transmission electron micrograph of Fig. 2, which was taken during the *in situ* experiment, suggests the same, however, on a smaller scale. The untransformed regions show strong electron microscopy contrasts, which are due to the small tilting of the pseudocubic axes between domains inside the colonies as well as between domains of different colonies. In the transformed regions, this tilt is, at least partly, removed. These regions appear, therefore, mostly in uniform contrast, usually as bright areas. Thus, the bright zone in Fig. 2 is not a crack but the transformed specimen region.

As described in Part I,[1] the microstructure of the crystals consists of tetragonal domains arranged in colonies preferably running in ⟨111⟩ directions. These colonies fill the whole volume, often in helical arrangements. Video records taken during *in situ* straining show that ferroelastic reorientation preferentially proceeds in the longitudinal direction of the colonies, where the switching speed is considerably higher than during a sidewise penetration of the transformation front into a colony. Since the colonies are extended along ⟨111⟩, their boundaries often appear in ⟨110⟩ directions within a {100} foil, thus explaining the above results.

For a closer inspection of the transformation or switching process, at first the colony structures designated by (a) in Section III of Part I[1] will be discussed. Here, those colonies adjoin each other, which are composed of domains with boundaries inclined to the foil surface. They alternately consist of variants t_1/t_2 and t_1/t_3, respectively. The symbols t_1, t_2, and t_3 are defined in Part I. The c-axis of t_1 was chosen in the direction of the foil normal, viz, parallel to the electron beam, and the c-axis of t_2 coincides with the tensile direction. When such a colony structure is transformed, variants t_1 and t_3 are reoriented; i.e., in every second colony, both domain variants change. The micrographs of Fig. 3 were taken of such a colony structure, the lower region of which (marked t_2) is already partially transformed, which can be deduced from the contrast behavior. As mentioned in Part I, in the untransformed region strong contrast arises at the domain boundaries so that it is not possible at the beginning to identify the domain variants unambiguously. In Fig. 3(a), colonies C_1 made of t_1/t_2 throughout appear bright

Fig. 2. HVEM micrograph taken during *in situ* straining at about 1150°C. The transformed region appears in bright contrast. The domain reorientation preferentially propagates in ⟨110⟩ directions. Foil orientation is close to the [100] pole.

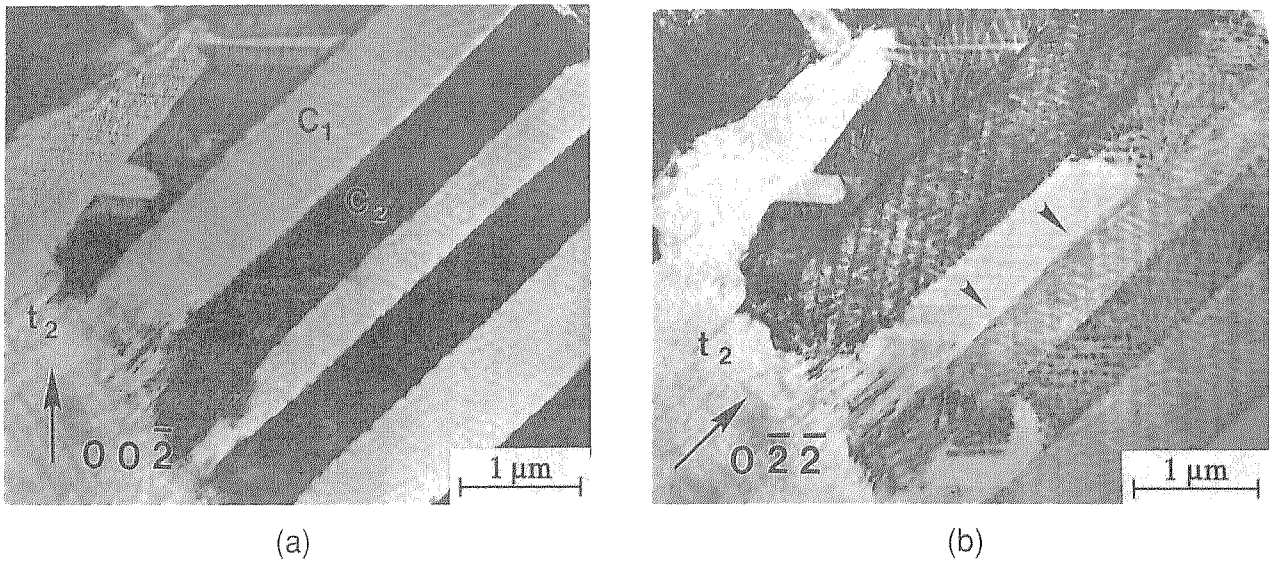

Fig. 3. Partially transformed colonies imaged with different g-vectors close to the [100] pole. (a) $\vec{g} = [00\bar{2}]$. (b) $\vec{g} = [0\bar{2}\bar{2}]$.

whereas colonies C_2 consisting of t_1/t_3 appear dark. Thus, it follows that the dark contrast must be assigned to variant t_3. At a different diffraction vector in Fig. 3(b), both colony types are almost uniformly dark, with the exception of one part of one colony C_2, marked by arrows. From the darkness of colonies C_1 and the fact that the transformed area in orientation t_2 appears bright in the lower part of the micrograph, it may be concluded that t_1 causes the dark contrast in Fig. 3(b). Consequently, in C_2 and marked by arrows, domain variant t_1 must already be transformed in that part of it, where variant t_3 still exists as known from Fig. 3(a). This behavior demonstrates that the transformation process need not continuously propagate from one domain to the next, but that it is nucleated in every individual domain.

In colony structure (b) of Part I, the adjoining colonies consist of domains t_1/t_2 and t_2/t_3 with an apparent [010] longitudinal extension of the colony, or of t_1/t_3 and t_2/t_3 with the colony in [001] extension. In the colonies with inclined domain boundaries, both domain variants can be reoriented if the longitudinal extension of the colonies is perpendicular to the tensile direction. However, in all types of adjoining colonies formed by domains with boundaries in edge-on orientation, only every second domain variant will be changed. These colonies do not

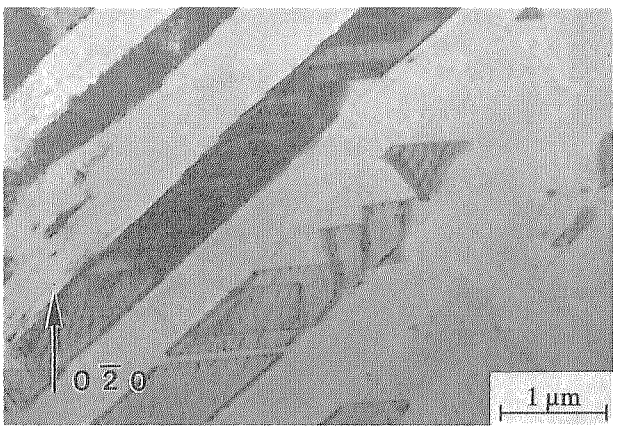

Fig. 5. Separated single tetragonal domains remaining unchanged while the main part (bright region) is reoriented during *in situ* straining. Some domains are partially transformed as indicated by their irregularly shaped lateral boundaries. Foil orientation is close to the [100] pole.

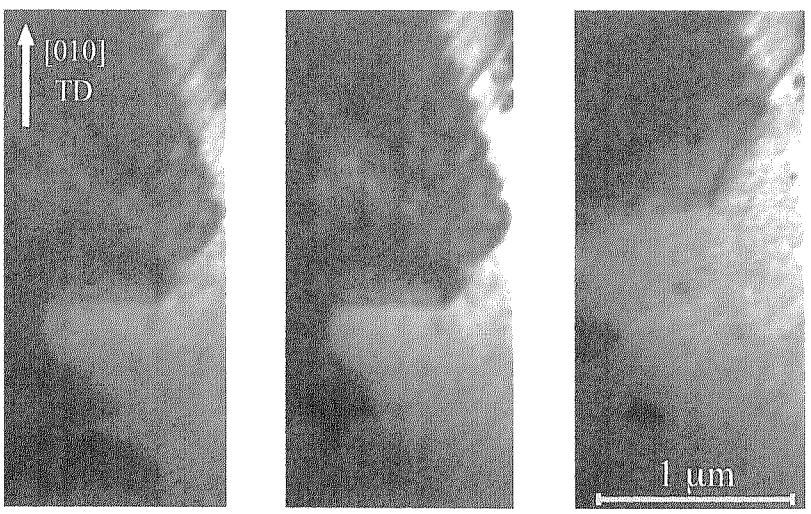

Fig. 4. Video tape recording of the reorientation process of domains during *in situ* straining. (a), (b), and (c) show subsequent frames. In (b) and (c), the missing contrast of single domains indicates the reorientation of the latter. (TD: tensile direction.)

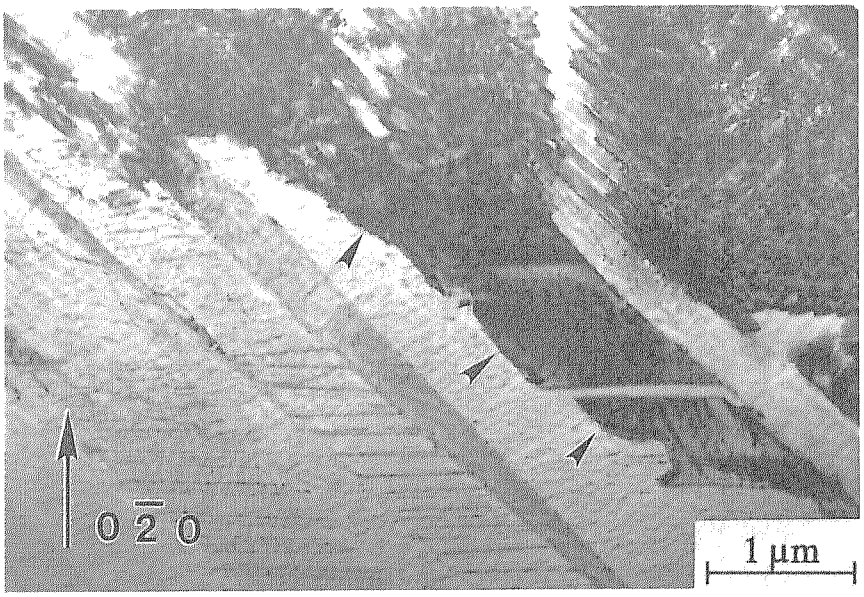

Fig. 6. Reoriented domains in the bright area on the lower left of the image. The thin lines in this region arise from residual defects. The boundary between reoriented and unchanged regions is marked by arrows. Foil orientation is close to the [100] pole.

show residual contrasts after transformation (see below) and are therefore difficult to analyze.

As mentioned above, the successive switching of domains within one colony proceeds rapidly, but this process can be time-resolved by means of video tape recording. In the video prints of Fig. 4, the contrast of a single domain vanishes from one print to the next within 1/50 s, indicating the reorientation of the domain. In contrast to that, the switching process inside the individual domains has not been resolved by subsequent video frames. However, in several cases intermediate stages of the domain reorientation are observed if the ferroelastic deformation stopped due to internal stress fields or an instantaneous change of the local stress, which may have been caused by deformation in the neighborhood. Figure 5 shows several platelike domains which are separated from the colony, thus remaining untransformed after straining. Some domains are not completely transformed, as irregularly shaped boundaries occur wherever the transformation front laterally penetrating into the platelike domains had stopped.

After the complete transformation, all domains have adopted the orientation of t_2. The transformed region resembles the single crystalline state, leaving, however, some kinds of residual contrasts and defects.

(2) *Residual Contrasts and Defects*

Three types of residual contrasts are observed in the completely transformed areas. They are (i) a surface relief, (ii) a misorientation between reoriented regions, and (iii) antiphase boundaries, and will now be described.

(i) Surface relief: Quite often, very fine lines of weak contrast perfectly reflect the domain and colony boundaries present before domain switching. While domains with boundaries arranged edge-on are hard to recognize after transformation, these structures occur inside colonies with inclined domain

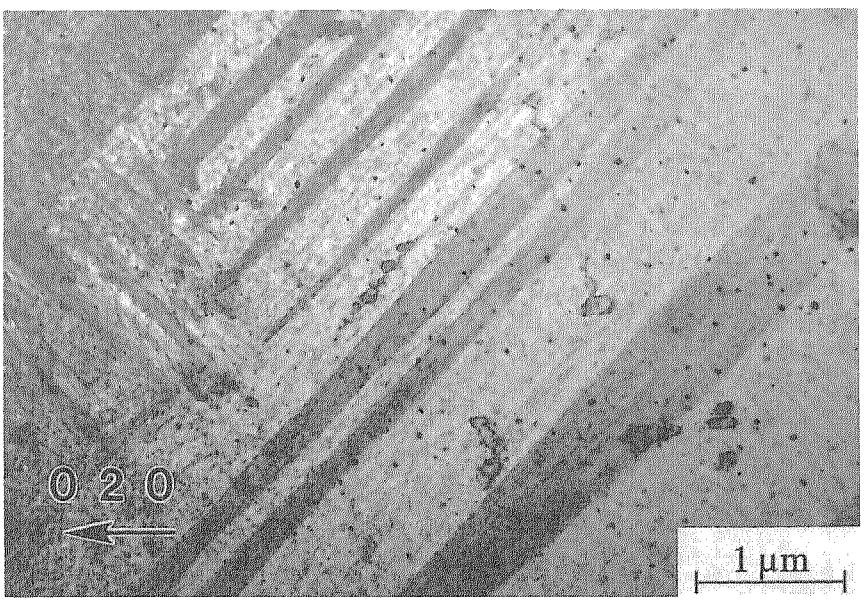

Fig. 7. Transformed region after *in situ* straining. The weak black–white contrast is caused by slightly tilted crystal regions. Foil orientation is close to the [100] pole.

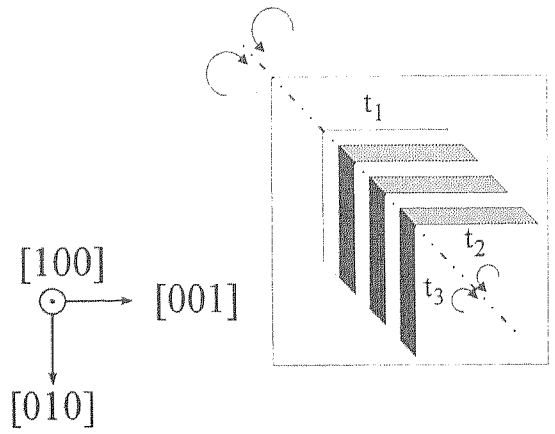

Fig. 8. Schematic drawing of the mutual tilt of colonies viewed in the direction of the electron beam. The figure refers to the colony structure labeled (a) in Part I.

boundaries. A typical example is shown in Fig. 6, where the residual contrast in the lower left part is obviously attributed to a surface relief arising during the reorientation of the domains. As described in Part I, the *c*-axes of different domains deviate slightly from their orthogonal orientation. The *c*-axes of the domains arranged edge-on are mutually tilted around an axis perpendicular to the surface, whereas those of the inclined domains are tilted around an axis parallel to the surface. In other words, in the first case the lattice distortions between the twinned domains occur exclusively in the foil plane, whereas for inclined domains, these distortions exhibit a component normal to the foil, resulting in a surface relief after reorientation or untwinning of the domains.

(ii) Misorientation between reoriented regions: Figure 7 presents a second type of residual distortions. Areas as large as the colonies and elongated in the ⟨110⟩ direction appear in dark or bright contrast, depending sensitively on the excitation conditions. The reason for this contrast is probably a mutual tilt of the colonies as a whole. As explained in Part I, for a better lattice accommodation contiguous colonies should mutually be tilted, as schematically shown by Fig. 8 for the colony configuration (a) of Part I. The colony boundary and therefore

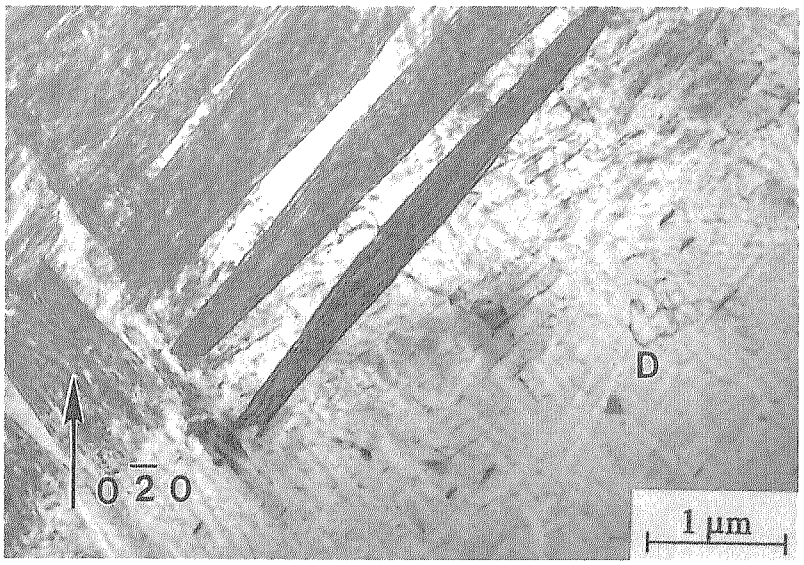

(a)

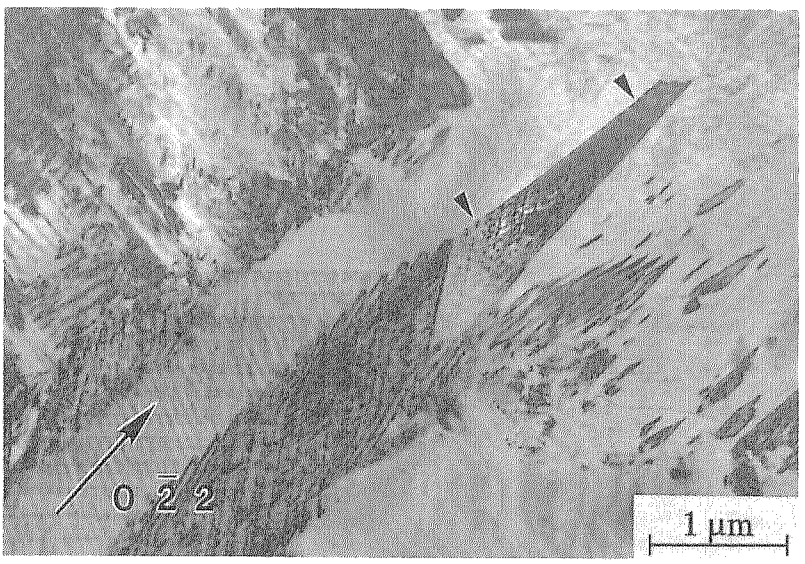

(b)

Fig. 9. Residual defects in different transformed regions after *in situ* straining. The fringe contrast arises from a kind of antiphase domain boundary (APB) owing to a fault in the up–down arrangement of the oxyen atoms. (a) APB's (dark) within the transformed region (D dislocation). (b) APB (arrows) at a colony boundary, but only in the transformed part of the colony. Foil orientation is near the [111] pole.

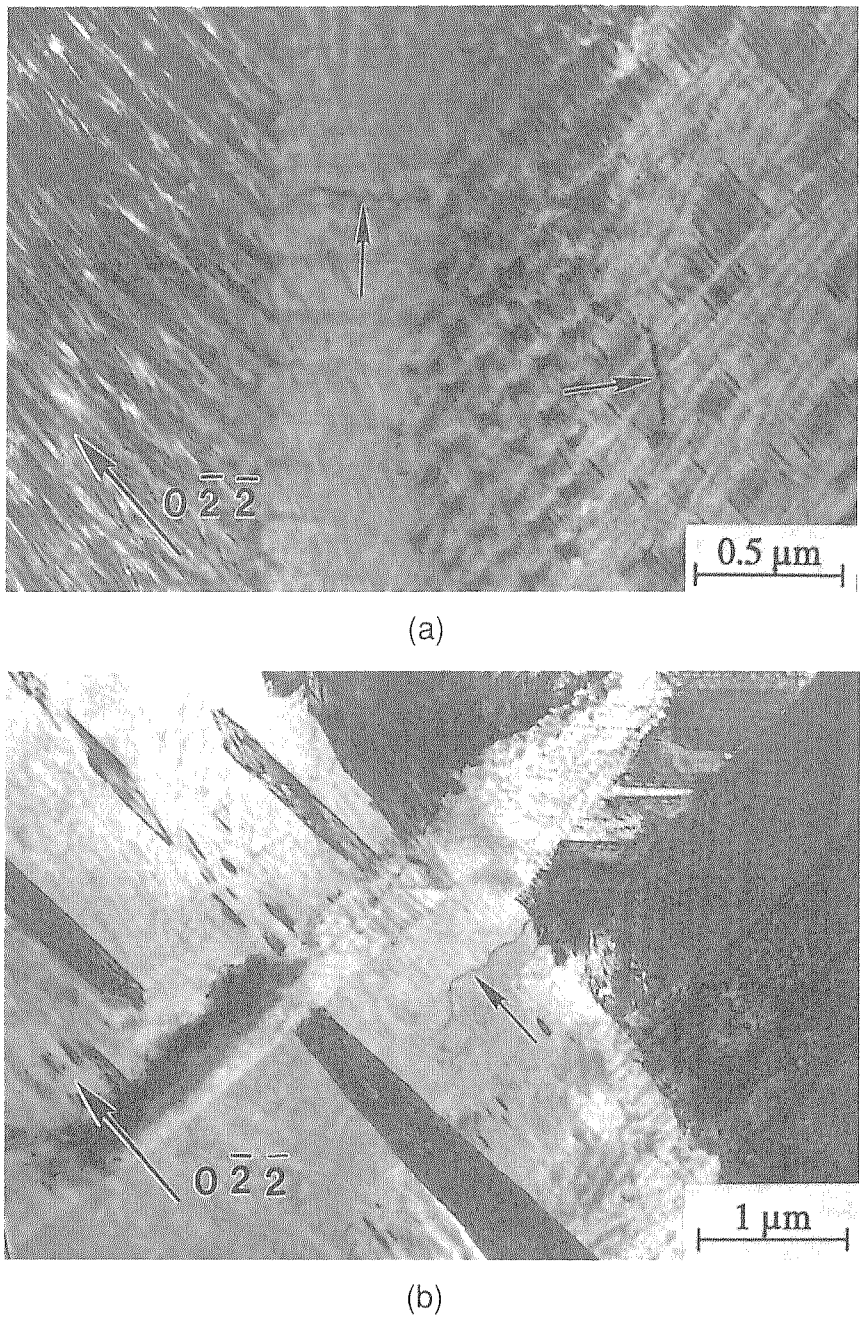

Fig. 10. Dislocations in t'-ZrO_2 marked by arrows. (a) Dislocations in the initial material, probably created during the ferroic cubic-to-t' phase transformation. Foil orientation is close to the [100] pole. (b) Deformation-induced dislocations after *in situ* straining. Foil orientation is close to the $[2\bar{1}1]$ pole.

the twin plane of the adjoining domains are perpendicular to the surface. The deviation of the domains from their orthogonal relationship is accommodated by a tilt between both colonies around an axis of ⟨111⟩ type in the colony boundary, sketched by the dashed–dotted line (compare Fig. 8 in Part I). By the transformation process, this tilt is reduced, which causes strains in the spatial arrangement of the colonies, which explain the black–white regions elongated in ⟨110⟩ directions as in Fig. 7.

(iii) Antiphase boundaries: The third category of residual defects are planar defects visualized by their fringe contrast. They again have the dimensions of colonies and are elongated in the ⟨110⟩ direction. Figure 9(a) shows examples of these defects inside the transformed region. In Fig. 9(b), the fringe contrast appears only in that part of the colony which is already transformed, marked by arrows. The same defects occur in deformed tetragonal ZrO_2. They were identified as a kind of antiphase domain boundaries (APB's) on {110} planes.[15] In that case, they arose during dislocation glide, causing a fault in the up–down arrangement of the oxygen atoms. In the present case these defects are not associated with the presence of dislocations. However, the same faults may arise when the transformation process starts from opposite sides, with transformed regions meeting which suffered a distinct lattice shift. Usually, the APB's arise at the colony boundaries; i.e., the transformation zones with different starting points have met there. APB's particularly often occur at colony boundaries oriented edge-on in the foil so that they become visible by their fringe contrast only if the specimen is tilted from the usual [100] orientation. This preferred existence at the boundaries oriented edge-on is probably due to the thin foil and the special deformation geometry. The different transformation zones need not necessarily meet at a colony boundary. In principle, the different crystal regions may adjoin at any place, so that the APB's are not restricted to planes, but may be curved, as tilting experiments

confirmed for the transformed part of the colony marked by arrows in Fig. 9(b).

(3) Dislocations

In addition to residual defects, dislocations also occur. There are many small segments prior to the straining experiment, but owing to the intense contrast of the domain boundaries they could rarely be imaged in untransformed material. Figure 10(a) gives an example of such preexistent dislocations, marked by arrows. Straining often causes dislocations to appear in colonies which are only partially transformed, especially near the boundary to the transformed part. Figure 10(b) shows such a type of dislocation indicating a connection between dislocation processes and domain switching. But up to now, it has not been possible to observe dislocation motion during the *in situ* experiments on t'-zirconia.

Macroscopic deformation experiments with strains exceeding the ferroelastic range showed extensive dislocation plasticity.[16] The dislocations then have to move not in the original polydomain tetragonal zirconia but in a transformed material which, in tension, is a tetragonal single crystal containing residual defects. As mentioned in the Introduction, ferroelastic domain switching was also observed in partially stabilized zirconia.[6] Besides, this material may have a tetragonal matrix rather than a cubic one,[6,15] which would follow from the phase diagram. These effects are not considered in the current literature on the plastic deformation of PSZ[7–10] but are briefly discussed in Ref. 5. Therefore, knowledge of the microstructure of tetragonal zirconia after ferroelastic deformation, including the residual defects, is a prerequisite of understanding the deformation behavior of the technically interesting two-phase partially stabilized zirconia materials.

IV. Conclusions

- *In situ* straining experiments in an HVEM at 1150°C allowed direct observation of domain switching during ferroelastic deformation of t'-ZrO_2.
- The electron microscopy contrasts in the deformed areas are interpreted on the basis of the detailed knowledge of the initial domain and colony structure investigated in Part I of this paper.
- Video recordings revealed the dynamics of the ferroelastic deformation. A transformation front propagates by successively reorienting individual domains into that variant with its c-axis parallel to the tensile direction. The front propagates preferentially in the ⟨111⟩ direction of the longitudinal extension of the colonies. Under tensile loading, a tetragonal single crystal is formed.
- The transformed area exhibits residual contrasts, originating from a surface relief and from misorientations between whole colonies, and residual defects, which should be identical with antiphase boundaries observed earlier in PSZ.
- Dislocations gliding after ferroelastic deformation must move in the transformed microstructure; i.e., they interact with the residual defects. These processes are most probably also important for the plastic deformation of PSZ.

Acknowledgment: The authors thank the staff of the Halle HVEM for keeping the instrument in good condition and for permanent help.

References

[1]D. Baither, B. Baufeld, U. Messerschmidt, A. Foitzik, and M. Rühle, "Ferroelasticity of t'-Zirconia: I, High-Voltage Electron Microscopy Studies of Morphology and Structure," *J. Am. Ceram. Soc.*, **80** [XX] XX–XX (1997).

[2]A. V. Virkar and R. L. K. Matsumoto, "Toughening Mechanism in Tetragonal Zirconia Polycrystalline (TZP) Ceramics"; pp. 653–63 in Advances in Ceramics, Vol. 24, *Science and Technology of Zirconia III*. Edited by S. Somiya, N. Yamamoto, and H. Yanagida. American Ceramic Society, Westerville, OH, 1988.

[3]C.-J. Chan, F. F. Lange, M. Rühle, J. F. Jue, and A. V. Virkar, "Ferroelastic Domain Switching in Tetragonal Zirconia Single Crystals—Microstructural Aspects," *J. Am. Ceram. Soc.*, **74**, 807–13 (1991).

[4]K. M. Prettyman, J.-F. Jue, A. V. Virkar, C. R. Hubbard, O. B. Cavin, and M. K. Ferber, "Hysteresity Effects in 3 mol% Yttria-Doped Zirconia (t'-Phase)," *J. Mater. Sci.*, **27**, 4167–74 (1992).

[5]U. Messerschmidt, D. Baither, B. Baufeld, and M. Bartsch, "Plastic Deformation of Zirconia Single Crystals: A Review," *Mater. Sci. Eng. A*, in press.

[6]B. Baufeld, D. Baither, U. Messerschmidt, and M. Bartsch, "High Voltage Electron Microscopy *in situ* Study on the Plastic Deformation of Partially Stabilized Tetragonal Zirconia," *Phys. Status Solidi (a)*, **150**, 297–306 (1995).

[7]A. Dominguez-Rodriguez, V. Lanteri, and A. H. Heuer, "High-Temperature Precipitation Hardening of Two-Phase Y_2O_3-Partially Stabilized ZrO_2 Single Crystals: A first report," *J. Am. Ceram. Soc.*, **69**, 285–87 (1986).

[8]A. H. Heuer, V. Lanteri, and A. Dominguez-Rodriguez, "High-Temperature Precipitation Hardening of Y_2O_3 Partially-Stabilized ZrO_2 (Y-PSZ) Single Crystals," *Acta Metall.*, **37**, 559–67 (1989).

[9]J. Martinez-Fernandez, M. Jimenez-Melendo, A. Dominguez-Rodriguez, K. P. D. Lagerlöf, and A. H. Heuer, "High-Temperature Precipitation Hardening of Y_2O_3 Partially-Stabilized ZrO_2 (Y-PSZ) Single Crystals—II. A Quantitative Model for the Hardening," *Acta Metall. Mater.*, **41**, 3171–80 (1993).

[10]J. Martinez-Fernandez, M. Jimenez-Melendo, A. Dominguez-Rodriguez, P. Cordier, K. P. D. Lagerlöf, and A. H. Heuer, "High-Temperature Precipitation Hardening of Y_2O_3 Partially-Stabilized ZrO_2 (Y-PSZ) Single Crystals—III. Effect of Solute Composition and Orientation on the Hardening," *Acta Metall. Mater.*, **43**, 2469–84 (1995).

[11]V. K. Wadhawan, "Ferroelasticity and Related Properties of Crystals," *Phase Transitions*, **3**, 3–103 (1982).

[12]A. Foitzik, M. Stadtwald-Klenke, and M. Rühle, "Ferroelasticity of t'-ZrO_2," *Z. Metallkd.*, **84**, 397–404 (1993).

[13]M. Hayashi, "Kinetics of Domain Wall Motion in Ferroelectric Switching. I. General Formulation," *J. Phys. Soc. Jpn.*, **33**, 616–28 (1972).

[14]U. Messerschmidt and M. Bartsch, "High-Temperature Straining Stage for *in situ* Experiments in the High-Voltage Electron Microscope," *Ultramicroscopy*, **56**, 163–71 (1994).

[15]D. Baither, B. Baufeld, and U. Messerschmidt, "Defect Formation during Plastic Deformation of Y_2O_3 Partially Stabilized ZrO_2 Single Crystals," *J. Am. Ceram. Soc.*, **78**, 1375–79 (1995).

[16]D. Baither, B. Baufeld, and U. Messerschmidt, unpublished results. □